



SCUOLA INTERNAZIONALE SUPERIORE DI STUDI AVANZATI

SISSA Digital Library

First-principles characterization of Mg low-index surfaces: Structure, reconstructions, and surface core-level shifts

Original

First-principles characterization of Mg low-index surfaces: Structure, reconstructions, and surface core-level shifts / Gunde, M.; Martin-Samos, L.; De Gironcoli, S.; Fanetti, M.; Orlov, D.; Valant, M.. - In: PHYSICAL REVIEW. B. - ISSN 2469-9950. - 100:7(2019), pp. 1-7. [10.1103/PhysRevB.100.075405]

Availability:

This version is available at: 20.500.11767/117282 since: 2021-01-14T14:58:40Z

Publisher:

Published

DOI:10.1103/PhysRevB.100.075405

Terms of use:

Testo definito dall'ateneo relativo alle clausole di concessione d'uso

Publisher copyright

note finali coverpage

(Article begins on next page)

First-principles characterization of Mg low index surfaces: structure, reconstructions and Surface Core Level Shifts

Miha Gunde^{1,2}, L. Martin-Samos^{1,3,*}, Stefano de Gironcoli⁴, Mattia Fanetti¹, Dmytro Orlov^{1,5}, Matjaz Valant^{1,6}

¹ *Materials Research Laboratory, University of Nova Gorica, Vipavska 11c 5270-Ajdovščina, Slovenija,*

² *Laboratory of Analysis and Architecture of Systems,*

CNRS and University Toulouse III-Paul Sabatier,

7 avenue du Colonel Laroche, F-31400, Toulouse, France

³ *CNR-IOM/Democritos National Simulation Center, Istituto Officina dei Materiali,*

c/o SISSA, via Bonomea 265, IT-34136 Trieste, Italy,

⁴ *SISSA, via Bonomea 265, IT-34136 Trieste, Italy,*

⁵ *Division of Materials Engineering, Department of Mechanical Engineering,*

Lund University, Ole Rmners vg 1, Lund 22363, Sweden. and

⁶ *Institute of Fundamental and Frontier Sciences,*

University of Electronic Science and Technology of China, Chengdu 610054, China

In this work, first-principles calculations provide structural characterization of three low index Mg surfaces — Mg(0001), Mg(10 $\bar{1}$ 0) and Mg(11 $\bar{2}$ 0) —, and their respective Surface Core Level Shifts (SCLS). Inspired by the close similarities between Be and Mg surfaces, we also explore the reconstruction of Mg(11 $\bar{2}$ 0). Through the calculation of surface energies and the use of angular-component decomposed DOS, we show that reconstructions are likely to occur at Mg(11 $\bar{2}$ 0) surface, similarly to what was found earlier for Be(11 $\bar{2}$ 0). Indeed, the surface energy of some of the explored reconstructions is slightly lower than that of the unreconstructed surface. In addition, because of lattice symmetry, the morphology of the unreconstructed surface (11 $\bar{2}$ 0) results in a step-like zig-zag chain packing, with topmost chains supporting a resonant, quasi-1D, partially filled electronic state. As the presence of partially filled quasi-1D bands is a necessary condition for Peierls-like dimerization, we verify that the un-dimerized surface chain remains stable with respect to it. Some of the reconstructions, namely the 2 \times 1 and 3 \times 1 Added Row (AR) reconstructions, induce a stronger relaxation of the topmost chains, increasing the coupling with lower layers and thus significantly damping the quasi-1D character of this state. The original approach followed offers a common and general framework to identify quasi-1D bands — even in the case of resonant electronic surface states — and to meaningfully compare calculated and measured SCLS even in the presence of multi-component peak contributions.

I. INTRODUCTION

In the modern age of high-performance yet sustainable material design, magnesium-based metals shine in both structural and functional applications. These include light-weight structural components in **vehicles** and electronics, bio-resorbable implants in medicine, and hydrogen storage materials for energy [1, 2], to name a few. The characteristics of magnesium enabling such applications are its low density (the lowest among structural metals) and its high chemical reactivity. The latter often also represents the main limiting factor, causing unacceptably high degradation rates [3]. Mitigating this is complicated, since degradation phenomena on magnesium surfaces are still poorly understood, especially at the atomic-scale level. The hexagonal close-packed lattice of Mg usually causes strong crystallographic texture development during fabrication, which calls for an in-depth investigation of low-index surface planes. Such deep understanding requires a detailed model of the pristine surface structure, including relaxations and reconstructions, as both will determine the physico-chemical properties of the surfaces.

Besides the aforementioned interest and related challenges in Mg applications, the fundamental study of Mg has been closely related to anomalies found in Be. Com-

parative studies between low-index surfaces of the two elements have found many similarities. Among others are, (i) the expansion of the 0001 surface layer [4–9] (in contrast with the traditional simple theory of metals [10]), (ii) the large multilayer relaxation, and (iii) the oscillatory thermal expansion of the (10 $\bar{1}$ 0) surface [11–14]. However, after the work of Cho *et al.* [11] in 2000, where Be(10 $\bar{1}$ 0) only was found to exhibit Surface Core Level Shift (SCLS) oscillations, Mg was relegated to the category of simple metals, thus reinforcing the idea that Be surface anomalies were to be ascribed to its semi-metallicity. The fundamental interest in Mg surfaces was not renewed until recently, despite Plummer *et al.* [13] reporting a remarkable oscillatory surface thermal expansion in both Mg(10 $\bar{1}$ 0) and Be(10 $\bar{1}$ 0) in 2001.

In addition to the aforementioned peculiarities, Be is the only simple metal known to reconstruct [15–17] in standard conditions, although very recently the reconstruction of a K surface under high tensile stress [18] was reported. This peculiarity is usually attributed to the atypical bonding nature of Be [19–21] that induces a band structure with energy gaps in a large portion of the Brillouin Zone near the Fermi energy, *i.e.* a band structure more prototypical of a semi-metal.

In 2016, Li *et al.* [22] challenged the idea that Dirac node lines are a peculiar feature of topological insula-

tors, by predicting their presence at the (0001) surface of Be and other alkali earth metals, including Mg. This revived the discussion about the importance of atomic arrangement over bonding nature.

In the present work, we use first-principles calculations to provide a full characterization of three low-Miller-index Mg surfaces, from structure to Surface Core-Level Shifts (SCLS), including possible reconstructions inspired by the similarities between Be and Mg surfaces. Our results predict that Mg(11 $\bar{2}$ 0) surface **may** reconstruct. Indeed, the surface energy of some of the explored reconstructions is slightly lower than the unreconstructed one. Because of the lattice symmetry, the morphology of the unreconstructed surface results in a step-like zig-zag chain packing, with the topmost chains supporting a resonant, quasi-1D, partially filled electronic state. The existence of a Peierls-like dimerization is ruled out by our calculations, verifying that the un-dimerized surface chain remains locally stable against it. On the other hand, some of the predicted reconstructions, namely the 2 \times 1 and 3 \times 1 Added Row (AR) reconstructions, induce a stronger relaxation of the topmost chains, increasing the coupling with the lower layers and thus destroying the quasi-1D character of the state. In addition, the approach **followed** provides a common and general framework to identify partially filled quasi-1D bands, even in the case of resonant surface states. We develop an original methodology to compute depth-weighted SCLS, allowing a meaningful comparison with measured SCLS when the surface exhibits multi-component peak contributions, as is the case for the predicted reconstructions.

II. COMPUTATIONAL APPROACH

The calculations presented in this work are based on Density Functional Theory (DFT) as implemented in the Quantum ESPRESSO distribution [23]. We adopt the Perdew-Burke-Ernzerhof (PBE) exchange-correlation functional [24] and ultrasoft pseudopotentials as provided in the PSLibrary [25] collection, namely the Mg.pbe-nl-rrkjus.UPF dataset. Wavefunctions and densities are expanded in a basis of plane waves up to a kinetic energy cutoff of 58 Ry and 358 Ry, respectively. Slabs of 11, 20 and 15 layers are used to model the Mg(0001), Mg(10 $\bar{1}$ 0) and Mg(11 $\bar{2}$ 0) surfaces, respectively, resulting in similar thicknesses. For the calculation of SCLS, a core-excited pseudo-potential was generated introducing a hole in the Mg 2p core state, assuming the same cutoff radii, projectors and hardness as the original Mg.pbe-nl-rrkjus.UPF. Atomic tests on the transferability and robustness of the generated pseudo-potential give an all-electron *vs* pseudo-potential error of less than 10 meV for excited atomic configurations up to 5 eV. In order to minimize interactions between periodic replicas in the Final-State SCLS calculations we used 3 \times 3, 3 \times 2 and 4 \times 4 surface supercells for Mg(0001), Mg(10 $\bar{1}$ 0) and Mg(11 $\bar{2}$ 0), respectively. With this choice, all cells have a compar-

	a (Å)	c/a
this work (PBE)	3.19	1.62
Ref. [27] (LDA)	3.12	1.62
Ref. [11] (LDA)	3.13	1.62
Ref. [28] (LDA)	3.11	1.62
Ref. [29] (LDA)	3.13	1.62
Ref. [29] (PBE)	3.20	1.62
Exp. [26]	3.21	1.62

TABLE I. Theoretical bulk equilibrium lattice parameters compared with literature values. For the cited theoretical references the exchange-correlation functional used (LDA or PBE) is specified. The experimental value (Ref. [26]) corresponds to the equilibrium lattice parameter of Mg measured at ambient temperature.

ble surface area of aspect ratio close to unity. Accordingly, the Brillouin zone (BZ) was sampled with an equivalent Monkhorst-Pack k-point mesh of 8 \times 8 for the periodic directions. Benchmark calculations on selected surface models have also been performed within the Local Density Approximation (LDA), see Supplementary Information. LDA pseudopotentials were generated with the same cutoff radii, projectors and hardness as Mg.pbe-nl-rrkjus.UPF, and displayed equivalent transferability and robustness.

III. SURFACE STRUCTURE AND SURFACE ENERGY

Magnesium crystallizes in the hexagonal close-packed (hcp) structure with lattice parameters $a = 320.9$ pm, $c = 521.0$ pm and $c/a = 1.62$ [26]. The three surfaces under investigation, Mg(0001), Mg(10 $\bar{1}$ 0) and Mg(11 $\bar{2}$ 0), are shown in Figure 1 (top and side views) together with the corresponding cutting plane in the unit cell of the respective HCP crystal. Table I reports the calculated values of the bulk equilibrium lattice parameters, obtained after a full relaxation using the computational approach described in the previous section.

	(0001)	(10 $\bar{1}$ 0)	(11 $\bar{2}$ 0)
d_{12}	2.63 (+1.2%)	0.73 (-19.2%)	1.47 (-7.2%)
d_{23}	2.60 (+0.2%)	2.01 (+8.0%)	1.65 (+4.5%)
d_{34}	2.59 (-0.1%)	0.81 (-10.7%)	1.58 (-0.4%)
d_{45}	2.59 (-0.2%)	1.94 (+4.4%)	1.59 (+0.4%)

TABLE II. Interlayer distances, d and deviation in % with respect to the equivalent ideal bulk distance for Mg(0001), Mg(10 $\bar{1}$ 0) and Mg(11 $\bar{2}$ 0). d_{ij} denotes the distance between the i^{th} and j^{th} layer. Layer 1 is the topmost layer.

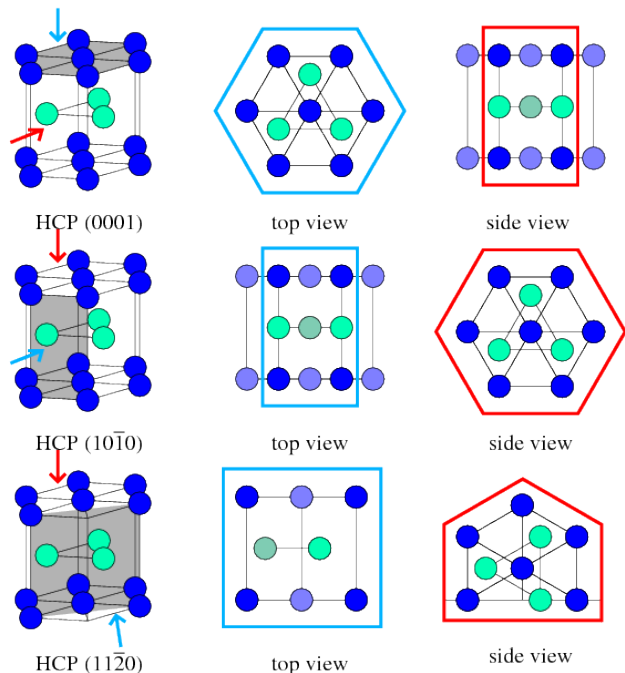


FIG. 1. Planes in the HCP crystal, side and top view of the three different Mg crystal surfaces.

In agreement with previous experimental and computational works [27–32], and similarly to Be(0001), the calculated distance between the topmost and second surface layer in Mg(0001) is larger than the bulk value, whereas variations of deeper interlayer distances are negligible, see Table II. The clear distinction between the topmost layer and deeper layers makes the identification of “surface atoms” and “bulk atoms” unambiguous in Mg(0001). The Mg(10 $\bar{1}$ 0) surface behaves quite differently, as can be seen from Table II. Two typical interlayer distances exist, a short one and a long one, resulting in the stacking of **bi-layers**. Compared to bulk values, the calculated first (short) interlayer distance is shorter while the second one is longer, resulting in an overall shrinking of the bi-layer together with an overall increase of the bi-layer-to-bi-layer distance. The most interesting difference between Mg(0001) and Mg(10 $\bar{1}$ 0) comes from the oscillations in the interlayer distances, already reported in Refs. [11, 12, 28, 32] and confirmed here (see also Table 1 from the Supplementary Information). The Mg(11 $\bar{2}$ 0) surface presents one characteristic interlayer distance. Because of the lattice symmetry, the morphology of the surface results in a step-like zig-zag chain packing. The overall relaxation effect, see Table II, is a shrinking of the first interlayer separation together with an increase

of the second one (see also Ref. [28]). However, contrary to Mg(10 $\bar{1}$ 0) but similarly to Mg(0001), the oscillations of the interlayer distances are negligible after the second layer.

Considering the reconstruction patterns explored by Stumpf *et al.* [21] for Be(11 $\bar{2}$ 0), we have explored 2 \times 1 and 3 \times 1 Added Row (AR) and Missing Row (MR) surfaces, as well as 4 \times 1 MR reconstructions for Mg(11 $\bar{2}$ 0). All results are summarised in Table III. The un-relaxed surface morphology with an Added/Missing Row appears as a series of Mg atomic chains along the [001] direction lying on an ideal Mg(11 $\bar{2}$ 0) substrate (see for instance Figure 2, comparing the unreconstructed surface with the 3 \times 1 AR reconstruction). The reconstructed surfaces exhibit a periodic corrugation. The symmetry reduction along the [010] direction makes the atomic relaxation along this direction slightly different depending on the lateral distance from the topmost atomic chains. This is more evident at the first layer atoms of the “substrate” and those of the second layer immediately underneath the chain. Two effects are competing: one is the expected inwards relaxation of interlayer distances for atoms that have a reduced number of neighbours along the direction perpendicular to the surface; the second is related to Friedel oscillations that induce inward or outward relaxations. In general, the oscillatory behaviour of interlayer distances is more pronounced than in the unreconstructed case. Interestingly, in the 2 \times 1 and 3 \times 1 AR structures the additional chain sits at an interlayer distance significantly shorter than in the unreconstructed case or in the other explored reconstructions. As a consequence, the coupling

	2X1	3X1 AR	3X1 MR	4X1 MR
d_{12}	1.39 (-11.9%)	1.39 (-11.9%)	1.45 (-8.5%)	1.47 (-7.2%)
d_{23}	1.70 (+7.7%)	1.70 (+7.7%)	1.65 (+3.8%)	1.65 (+3.8%)
d_{34}	1.53 (-2.9%)	1.53 (-2.9%)	1.58 (-0.2%)	1.58 (-0.1%)
d_{45}	1.60 (+1.0%)	1.61 (+1.0%)	1.57 (-1.1%)	1.59 (-0.01%)

TABLE III. Interlayer distances, d and deviation in % with respect to the equivalent ideal bulk distance for Mg(0001), Mg(10 $\bar{1}$ 0) and Mg(11 $\bar{2}$ 0) (the deviation with respect to bulk distances are calculated with full accuracy (double precision), variations between the reported % and distances are due to rounding errors). d_{ij} denotes the distance between the i^{th} and j^{th} layer. The topmost chain(s) has index 1. The atomic configuration for 2 \times 1 symmetry is identical for MR or AR.

between the topmost chain and the underlying layers is expected to be stronger for the 2 \times 1 and 3 \times 1 AR reconstructions than for all other surface morphologies, and this has consequences for the surface electronic structure (see later).

Our calculated surface energies are reported in Table IV, together with some results from literature. In Ref. [28] the surface energy of Mg(0001) was found to be significantly lower than for the other two surfaces (see

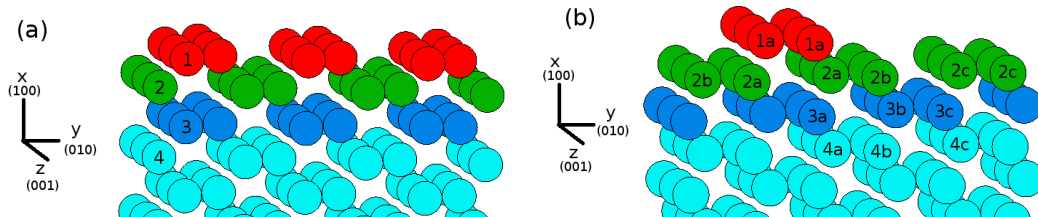


FIG. 2. Structure of the unreconstructed (a) and 3×1 AR reconstructed (b) $\text{Mg}(11\bar{2}0)$ surface. Topmost Mg chains are highlighted in red.

also Ref. [27, 30, 31, 33] for other LDA values), and our calculations confirm this trend. The Authors of Ref. [28] speculated about the possible stabilization of $\text{Mg}(10\bar{1}0)$ and $\text{Mg}(11\bar{2}0)$ surfaces through reconstruction and/or defect formation driven by surface stress. Indeed, according to Payne *et al.* [34], both surfaces exhibit a value for one of the surface-stress components (multiplied by the surface area per atom) larger than the bulk cohesive energy, satisfying a proposed criterion for structural instability. However, as reconstruction was not observed in $\text{Mg}(10\bar{1}0)$ [11], the authors concluded, for both $(10\bar{1}0)$ and $(11\bar{2}0)$ surfaces, that the stabilization should arise from the presence of defects. From our calculations, however, the presence of reconstructions at $\text{Mg}(11\bar{2}0)$ can not be ruled out as some of the reconstructed surfaces exhibit a surface energy slightly lower than the unreconstructed surface, with quasi-degenerate values. This result is robust with respect to the choice of the exchange and correlation functional (see Table 3 from the Supplementary Information). Surfaces with a high concentration of isolated adatoms/vacancies have clearly higher surface energies. The behaviour of $\text{Mg}(11\bar{2}0)$ surfaces with respect to reconstructions is very similar to what was found for the $\text{Be}(11\bar{2}0)$ surface [15, 16] which is known to display a 3×1 reconstruction.

IV. ELECTRONIC STRUCTURE

The origin of the reconstruction in the $(11\bar{2}0)$ surface can be traced back to the high surface energy of the unreconstructed surface. On the sole basis of the surface energy, we can predict that 2×1 and/or 3×1 AR reconstructions **may** occur. A closer analysis of the surfaces electronic structure and, in particular, of the atom-projected density of states (DOS) provides some additional arguments in favour of the aforementioned reconstructions. The total DOS of the three surface slabs exhibits the expected \sqrt{E} behaviour typical of a 3D nearly-free electron metal. The surface-atom projected DOS would be expected to exhibit a similar behaviour, possibly turning toward a flat dependence typical of 2D nearly-free electrons. Indeed, this is what we observe for all three surfaces, for the angular-projected components s , $2p_z$ and $2p_y$ that are co-planar with the surface planes. Surprisingly, only the $2p_y$ -projected DOS (see Fig. 3a)) of

	(0001)	(10 $\bar{1}0$)	(11 $\bar{2}0$)
t.w.	30	38	45
Ref. [28]	40	44	53
Ref. [29]	35	-	-
Reconstructed (11 $\bar{2}0$)			
2×1	3×1 AR	3×1 MR	4×1 MR
44	44	45	47
Add/Missing Atom at (11 $\bar{2}0$)			
3×1 MA	4×1 MA	2×1 AA	3×1 AA
48	47	49	48

TABLE IV. Calculated surface energy ($\text{meV}/\text{\AA}^2$) for the three unreconstructed surfaces (001,100 and 110) and for the Missing Row (MR) or Added Row (AR) reconstructions with different symmetry on $\text{Mg}(11\bar{2}0)$. The atomic configuration for 2×1 symmetry is identical for MR or AR. To compare with previous ideas [28] that the $\text{Mg}(11\bar{2}0)$ might be stabilized by the presence of point defects, the 3×1 and 4×1 Missing Atom (MA) and 2×1 and 3×1 Added Atom (AA) surface energies are also reported. "t.w." is used to indicate the results obtained in this work.

the unreconstructed $\text{Mg}(11\bar{2}0)$ surface strongly deviates from a \sqrt{E} or constant behaviour with a series of peaks around 1 eV below (and slightly above) the Fermi energy. These peaks **are reminiscent** of the energy levels of free electrons confined in a finite cylindrical potential well (see Ref. [35]), with energy values depending on a principal quantum number, $n = 1, 2, \dots$, and an angular (cylindrical) quantum number, $m = 0, 1, 2, \dots$. In the limit of **an infinitely deep** potential well, these tend to the n^{th} zeros ($z_m^{(n)}$) of the J_m Bessel function. The finite **depth** of the well shrinks the peaks to lower energies (see dot-dashed vertical red lines in Figure 3). Identical features have been observed in nano-wires (see Fig. 3 of Ref. [36]). Top layer Mg atoms in the ideally terminated $\text{Mg}(11\bar{2}0)$ surface form zig-zag chains along the $[001]$ crystallographic direction, that supports a partially filled, quasi-1D, surface-localized band originating from the overlap of Mg $2p_x$ orbitals. The resonant character of this band makes it difficult to precisely quantify its dispersive character in the k -resolved surface band-structures (k -resolved pDOS), while its signature is easily

observed in the angular-component decomposed pDOSs, see in Fig. 3.

As the presence of a partially filled quasi-1D band is a necessary condition for the existence of a Peierls-type dimerization, we performed calculations doubling the cell dimension along the zig-zag chains (along z) and forcing a starting configuration with Mg-Mg bond alternation. Surprisingly, the dimerized surface was found to be unstable, and to relax back to the ideal un-dimerized case. Therefore, our calculations rule out the Peierls mechanism as possible driving force for the reconstruction.

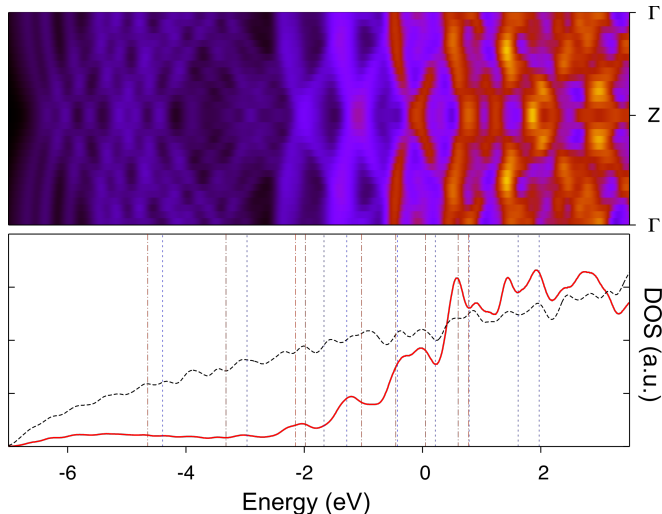


FIG. 3. Total p-DOS (black-dashed line), p_y projection at 1st layer atom of the unreconstructed Mg(1120) surface (red-continuous line), and k-resolved p_y density of states. Vertical dashed lines indicate the first nine quantized energy levels for 3D electrons in a cylindrical potential well with finite (red dot-dashed lines) and infinite (blue dashed lines) depth. For the finite depth case, a $\nu = 10$ value has been used, see Equation 3 of Ref. [35].

Among the investigated reconstructions, the peak structure in the p-DOS disappears for the 2×1 and 3×1 AR reconstructions, while the peaks are still present in the orbital-resolved $2p_y$ component of the 3×1 and 4×1 MR reconstructions. As previously mentioned, the inward relaxation of the topmost chains in the 2×1 and 3×1 AR is significantly larger than that in the other explored reconstructions, see Table III. This strengthens the coupling between the chain and the “substrate” layers, thus reducing the quasi-1D character of the electronic structure associated to the chain, and consequently reducing the high surface metallicity originated from the quasi-1D state.

Considering both the predicted **slightly** favourable surface energies and the increased coupling of the surface chain with the substrate, we predict that the most probable candidates for the reconstruction of Mg(1120) are the 2×1 and/or 3×1 AR. This is similar to the case of Be(1120), that has been reported to reconstructs with a

3×1 symmetry [15], most probably by the AR mechanism [21].

V. SURFACE CORE LEVEL SHIFTS

Core-level spectroscopy is an element-specific, environment-sensitive probe of a material. As such, it has been extensively employed in surface science investigations [16, 37] and used to address even subtle structural properties when sufficient resolution can be attained [13]. We report here our theoretically predicted surface core-level shifts for the Mg surfaces **investigated**, comparing with the few available experimental results. First of all, in agreement with previous works on

Layers	(0001)	(10 $\bar{1}$ 0)	(11 $\bar{2}$ 0)
12	+130	+110	+170
23	+0	+50	+10
34	-10	-20	-0
45	-10	+50	+10
XPS Δ_{B-S} [38]	140	-	-

TABLE V. Individual-layer calculated SCLSs (meV) for Mg(0001), Mg(10 $\bar{1}$ 0) and unreconstructed Mg(11 $\bar{2}$ 0). The numerical error is estimated to be of the order of 10 meV and accounts for the overall convergence parameters and the robustness of the ad-hoc generated core-hole pseudo-potential. ij denotes the i^{th} and j^{th} layer with 1 being the topmost layer. XPS Δ_{B-S} is an experimentally determined SCLS, with Δ_{B-S} being the energy difference at peak maximum between the fitted Bulk (B) and Surface (S) component.

(Mg(0001) [32, 38], Mg(10 $\bar{1}$ 0) [12]), the calculated SCLSs for the top to second layer in all three unreconstructed surfaces are positive and well separated from the others shifts (see Table V). Calculated SCLS for the Mg(0001) are in very good agreement with the measured value of 140 meV in Ref. [38] and converge very fast to the bulk value. To the best of our knowledge, experimental values for surface core-level shifts for the other two surfaces have not been reported in the literature yet.

It is worth noting that, contrary to what reports Ref. [12], our calculations display **SCLS** oscillations for Mg(10 $\bar{1}$ 0) surface, which is similar to that for the Be(10 $\bar{1}$ 0) surface, regardless of the flavour of the exchange-correlation functional used (see Table 2 from the Supplementary Information). As a consequence of the distinct multi-component contributions of the SCLS in Mg(10 $\bar{1}$ 0), reported in Table V, the assignment of the position of the “Bulk” peak in experimental XPS spectra might not be straightforward, especially if the experimental resolution is limited. As such, a meaningful comparison between theoretical and experimental SCLS will depend on the penetration depth of the XPS probe and the overall resolution of the experimental set-up.

In the case of the unreconstructed $(11\bar{2}0)$, similarly to the (0001) surface, a well defined surface peak is predicted with a quite large shift of 170 meV with respect to the second layer and very little depth dependence.

2×1			
Layers	a	b	c
1	+130	-	-
2	+38	+147	-
3	-17	+2	-
4	-18	+0	-
3×1 AR			
1	+150	-	-
2	+60	+160	+190
3	+10	+10	+50
4	+10	+10	+20

TABLE VI. Individual-layer calculated SCLSs (meV) for reconstructed 2×1 and 3×1 AR Mg($11\bar{2}0$) taking as reference the total energy of a deep Mg atom with a hole in the core. The numerical error is estimated to be of the order of 10 meV and accounts for the overall convergence parameters and the robustness of the ad-hoc generated core-hole pseudopotential. i denotes the i^{th} layer along the (100) direction and a , b or c refers to site positions along (010) , with $1a$ being the atoms from the topmost layer (the top most chain), see Figure 2. Because of symmetry 'c' sites are equivalent to 'b' sites in $2X1$.

In the case of the predicted AR reconstructed $(11\bar{2}0)$ surface models, the situation is more complex, since a number of different values for the SCLS are computed in the first few layers as a function of the relative position of the near-surface atom with respect to the added row. In Table VI the calculated core-level shift of near-surface atoms with respect to a bulk reference atom, located close to the center of the surface slab, are collected (see Fig. 2b for the labelling of the different surface atoms). Two broad regions can be distinguished: on one end a number of contributions are below 50-60 meV from the reference bulk atoms; unless very high resolution spectra can be acquired, these are likely to contribute to the "Bulk" peak, with different weights depending on the penetration depth of the impinging light and escape length of the outgoing electrons. On the other end contributions in the 130-190 meV range will determine a multi-component "Surface" peak. Similarly to Mg($10\bar{1}0$) surface, the value of the "S-B" core-level shift to be observed in an XPS experiment on Mg($11\bar{2}0$) is difficult to predict as it will critically depend on the penetration depth and the experimental resolution. We can however give a rough estimate of this difference that might help to discriminate between reconstructed and unreconstructed surfaces. We first impose a Gaussian broadening to each individual-layer SCLS; we then choose a penetration depth value between 3\AA and 5\AA : each Gaussian

is multiplied by an exponential decay, e^{-d_{1n}/δ_p} , with d_{1n} being the distance between the n^{th} layer and the topmost layer and δ_p being the penetration depth. The Gaussian returns the value of 1 when the topmost layer contributes with a single-component SCLS. We then calculate the core-level energy difference between "S" and "B" peaks (Δ_{S-B}) from the difference between peak maxima, see Figure 4. Δ_{S-B} are dependent of the penetration depth only in the case of multi-component contributions. Calculated Δ_{S-B} for the unreconstructed surfaces are 130, 120 and 170 meV for Mg(0001), Mg($10\bar{1}0$) and Mg($11\bar{2}0$), respectively. The calculated Δ_{S-B} for the 2×1 and 3×1 AR reconstructions are between 120-130 meV and 140-150 meV, depending on the chosen penetration depth. In spite of the uncertainty originating from the penetration depth definition, the difference between the resulting Δ_{S-B} for the reconstructed and the unreconstructed surface is significant; no less than 20-30 meV. Moreover, as the "Surface" peak of the reconstructed $(11\bar{2}0)$ is multi-component, contrary to the corresponding peak of (0001) and $(10\bar{1}0)$ surfaces, it exhibits an intrinsic broadening. In a high resolution XPS experiment it would be possible to determine whether the Mg($11\bar{2}0$) surface is reconstructed or not from the position and the apparent broadening of the surface peak.

VI. CONCLUSIONS

We have studied by first-principles calculations the structural and the SCLS properties of three low index surfaces of Magnesium. We found SCLS oscillations at Mg($10\bar{1}0$) surface analogous to the ones previously reported for Be($10\bar{1}0$) and more favourable surface energies for reconstructed Mg($11\bar{2}0$) surfaces, again similar to the behaviour previously reported for Beryllium. Moreover, from angular-component decomposed DOS (PDOS), we found that the unreconstructed Mg($11\bar{2}0$) surface is electronically unstable. The use of pDOSes provides a simple indicator of the quasi-1D character of the surface state even when the involved band is only a resonance. This kind of representation can, therefore, be used to theoretically predict the existence of such instabilities that may drive to reconstructions and/or Charge Density Wave phases. Due to their lower surface energy and the lifting of the electronic instability, the 2×1 and the 3×1 AR reconstructions (or a mixture of the two) are good candidates for Mg($11\bar{2}0$) surface morphology, similarly to Be($11\bar{2}0$) that reconstructs with a 3×1 periodicity. Our results show the strong similarities between Be and Mg surfaces and highlight the role of the lattice and the underlying atomic arrangements over peculiar bonding features.

We are grateful to Prof. Paolo Giannozzi, Prof. Alice Ruini and Dr. Luigi Giacomazzi for useful discussions. We also acknowledge Prof. Erio Tosatti for his advice during the preparation of the manuscript. The computer time was mainly provided by CINECA through

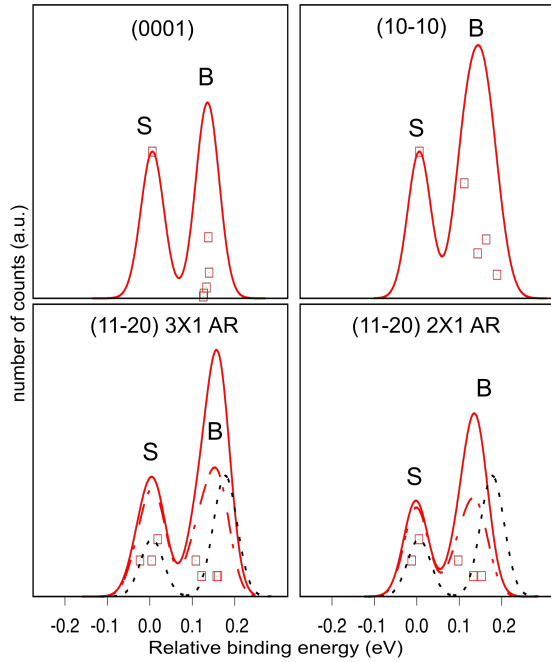


FIG. 4. Depth-weighted SCLSs for Mg(0001), Mg($10\bar{1}0$) and for 2X1 and 3X1 AR reconstructions at Mg(11-20), red solid lines, and for the un-reconstructed Mg($11\bar{2}0$), black dotted lines, for a penetration depth of 5 Å. For the reconstructed surfaces, depth-weighted SCLS at a penetration depth of 3 Å are also shown (red dash-dotted lines). The energies have been aligned to the surface peak maxima (S) of the (0001) surface. Red squares mark the position of individual layer SCLS. Their respective height corresponds to the intensity of the exponential decay, e^{-d_{1n}/δ_p} , with d_{1n} being the distance between the n^{th} layer and the topmost layer, and δ_p being the penetration depth. The Gaussians have a broadening of 50 meV.

IsC44 HP10CQGOFM project. This work has received funding from the EU-H2020 research and innovation programme under grant agreement No 654360 having benefitted from the access provided by CNR-IOM in Trieste (Italy) within the framework of the NFFA-Europe Transnational Access Activity. The support by the Slovenian Research Agency (Research Core Funding No. P2-0377 and Project Funding No. J2-7157) and Biomag project is also acknowledged.

-
- [1] K. N. S. Dmytro Orlov, Vineet V Joshi and N. R. Neelameggham, eds., *Magnesium Technology 2018* (Springer, TMS (Metals and Materials Society), 2018).
- [2] T. M. Pollock, *SCIENCE* **328**, 986 (2010).
- [3] M. Esmaily, J. E. Svensson, S. Fajardo, N. Birbilis, G. S. Frankel, S. Virtanen, R. Arrabal, S. Thomas, and L. G. Johansson, *PROGRESS IN MATERIALS SCIENCE* **89**, 92 (2017).
- [4] H. DAVIS, J. HANNON, K. RAY, and E. PLUMMER, *PHYSICAL REVIEW LETTERS* **68**, 2632 (1992).
- [5] P. Sprunger, L. Petersen, E. Plummer, E. Laegsgaard, and F. Besenbacher, *SCIENCE* **275**, 1764 (1997).
- [6] K. Pohl, J. Cho, K. Terakura, M. Scheffler, and E. Plummer, *PHYSICAL REVIEW LETTERS* **80**, 2853 (1998).
- [7] M. Lazzeri and S. de Gironcoli, *PHYSICAL REVIEW LETTERS* **81**, 2096 (1998).
- [8] I. Vobornik, J. Fujii, M. Hochstrasser, D. Krizmanic, C. E. Viol, G. Panaccione, and S. Fabris, *PHYSICAL REVIEW LETTERS* **99** (2007), 10.1103/PhysRevLett.99.166403.
- [9] In 1985, J. C. Boettger and S. B. Trickey, *Phys. Rev. B* **32**, 1356 (1985), predicted a large expansion of a beryllium dilayer.
- [10] J. INGLESFIELD, *REPORTS ON PROGRESS IN PHYSICS* **45**, 223 (1982).
- [11] J. Cho, Ismail, Z. Zhang, and E. Plummer, *PHYSICAL REVIEW B* **59**, 1677 (1999).
- [12] J. Cho, K. Kim, S. Lee, M. Kang, and Z. Zhang, *PHYSICAL REVIEW B* **61**, 9975 (2000).
- [13] Ismail, E. Plummer, M. Lazzeri, and S. de Gironcoli, *PHYSICAL REVIEW B* **63** (2001), 10.1103/PhysRevB.63.233401.
- [14] M. Lazzeri and S. de Gironcoli, *PHYSICAL REVIEW B* **65** (2002), 10.1103/PhysRevB.65.245402.
- [15] J. HANNON, E. PLUMMER, R. WENTZCOVITCH, and P. LAM, *SURFACE SCIENCE* **269**, 7 (1992).
- [16] L. JOHANSSON, H. JOHANSSON, E. LUNDGREN, J. ANDERSEN, and R. NYHOLM, *SURFACE SCIENCE* **321**, L219 (1994).
- [17] There is a controversy on a reported Al reconstruction,

- see R. LUDEKE and G. LANDGREN, PHYSICAL REVIEW LETTERS **47**, 875 (1981) never confirmed nor experimentally nor by independent theoretical calculations, see also footnote number 49 in Ref. [21]
- [21] F. Yin, S. Kulju, P. Koskinen, J. Akola, and R. E. Palmer, SCIENTIFIC REPORTS **5** (2015), 10.1038/srep10165.
- [19] T. LOUCKS and P. CUTLER, PHYSICAL REVIEW **133**, A819+ (1964).
- [20] M. CHOU, P. LAM, and M. COHEN, PHYSICAL REVIEW B **28**, 4179 (1983).
- [21] R. Stumpf, J. B. Hannon, P. J. Feibelman, and W. E. Plummer, "The unusual properties of the beryllium surface," (2005).
- [22] R. Li, H. Ma, X. Cheng, S. Wang, D. Li, Z. Zhang, Y. Li, and X.-Q. Chen, PHYSICAL REVIEW LETTERS **117** (2016), 10.1103/PhysRevLett.117.096401.
- [23] P. Giannozzi, S. Baroni, N. Bonini, M. Calandra, R. Car, C. Cavazzoni, D. Ceresoli, G. L. Chiarotti, M. Cococcioni, I. Dabo, A. Dal Corso, S. de Gironcoli, S. Fabris, G. Fratesi, R. Gebauer, U. Gerstmann, C. Gougoussis, A. Kokalj, M. Lazzeri, L. Martin-Samos, N. Marzari, F. Mauri, R. Mazzarello, S. Paolini, A. Pasquarello, L. Paulatto, C. Sbraccia, S. Scandolo, G. Sclauzero, A. P. Seitsonen, A. Smogunov, P. Umari, and R. M. Wentzcovitch, JOURNAL OF PHYSICS-CONDENSED MATTER **21** (2009), 10.1088/0953-8984/21/39/395502.
- [24] J. Perdew, K. Burke, and M. Ernzerhof, PHYSICAL REVIEW LETTERS **77**, 3865 (1996).
- [25] A. Dal Corso, COMPUTATIONAL MATERIALS SCIENCE **95**, 337 (2014).
- [26] C. Kittel, *Introduction to Solid State Physics* (Wiley, 2004).
- [27] A. WRIGHT, P. FEIBELMAN, and S. ATLAS, SURFACE SCIENCE **302**, 215 (1994).
- [28] P. Staikov and T. Rahman, PHYSICAL REVIEW B **60**, 15613 (1999).
- [29] J. Da Silva, C. Stampfl, and M. Scheffler, SURFACE SCIENCE **600**, 703 (2006).
- [30] P. SPRUNGER, K. POHL, H. DAVIS, and E. PLUMMER, SURFACE SCIENCE **297**, L48 (1993).
- [31] Ismail, P. Hofmann, A. Baddorf, and E. Plummer, PHYSICAL REVIEW B **66** (2002), 10.1103/PhysRevB.66.245414.
- [32] J.-J. Tang, X.-B. Yang, L. OuYang, M. Zhu, and Y.-J. Zhao, JOURNAL OF PHYSICS D-APPLIED PHYSICS **47** (2014), 10.1088/0022-3727/47/11/115305.
- [33] R. MONNIER and J. PERDEW, PHYSICAL REVIEW B **17**, 2595 (1978).
- [34] M. PAYNE, N. ROBERTS, R. NEEDS, M. NEEDELS, and J. JOANNOPOULOS, SURFACE SCIENCE **211**, 1 (1989).
- [35] X. Leyronas and M. Combescot, SOLID STATE COMMUNICATIONS **119**, 631 (2001).
- [36] Y. Tian, M. R. Sakr, J. M. Kinder, D. Liang, M. J. MacDonald, R. L. J. Qiu, H.-J. Gao, and X. P. A. Gao, NANO LETTERS **12**, 6492 (2012).
- [37] S. Lizzit, K. Pohl, A. Baraldi, G. Comelli, V. Fritzsche, E. Plummer, R. Stumpf, and P. Hofmann, PHYSICAL REVIEW LETTERS **81**, 3271 (1998).
- [38] R. KAMMERER, J. BARTH, F. GERKEN, C. KUNZ, S. FLODSTROM, and L. JOHANSSON, PHYSICAL REVIEW B **26**, 3491 (1982).